Suplemento de la Revista Mexicana de Física **3** 0308009 (2022) 1–7

Hadron research with AMBER at CERN

Jan Friedrich

TU Munich for the AMBER Collaboration.

Received 15 January 2022; accepted 6 May 2022

The recently approved NA66/AMBER experiment (Apparatus for Meson and Baryon Experimental Research) at the CERN Super Proton Synchrotron pursues a broad research program in quantum chromodynamics. It ranges in its first phase from a precision measurement of the proton radius with a 100 GeV muon beam to investigating the quark-gluon structure of mesons in Drell-Yan processes. In a second phase, radio-frequency separated kaon beams will allow to extend such investigations to the strangeness sector.

Keywords: Fixed-target experiment; muon and hadron beams; hadron structure.

DOI: https://doi.org/10.31349/SuplRevMexFis.3.0308009

1. Introduction

The various ways to learn experimentally about quantum chromodynamics (QCD) in hadrons reach from inclusive reactions, with hard quark-quark and quark-gluon collisions, to softer reactions in which resonances are obtained by the excitation of beam hadrons in gracing collisions, and to elastic scattering, in which the internal QCD structure is visible in terms of form factors.

In all approaches and theoretical descriptions, a core parameter is the mass of the hadronic system. For the low-lying states there is the most striking feature of the mass ratio between the pion, with a valence light-quark-antiquark structure, and the proton, with a valence three-quark structure, of about one-to-seven. This points to a very different way those systems are composed by its constituents. It is well established that a driving principle is chiral symmetry, linked to almost vanishing masses of the light quarks compared to the total mass of the bound systems. The breaking of this symmetry turns out very differently for the proton and the pion, as indicated in Fig. 1. While the proton has almost its entire mass still in the chiral limit of massless quarks, the pion turns massless itself in that limit, being identified as Nambu-Goldstone (NG) modes of the strong-interaction potential. The surplus of mass in case of the proton must lie in the mechanism by which mass is generated out of the strong binding, *i.e.* the emergence of hadron mass (EHM). Quantitatively, the standard model mass-generating mechanism via the coupling to the Higgs boson alone plays only a small role in the hadrons, indicated by the golden segments of the rings which represent the composition of the total hadron masses. The remaining part is either due to interference of the Higgs mechanism with the emergent mass generation (red), or exclusively due to EHM (blue). The latter part is missing for the NG modes, making the interference between EHM and Higgs contributions dominant. The kaon, with its heavier strange quark content, has a correspondingly larger contribution from the Higgs mechanism. Studying the parton distribution functions (PDF) and the global properties of these mesons thus gives best access to understand the mass emergence mechanism by the strong interaction.

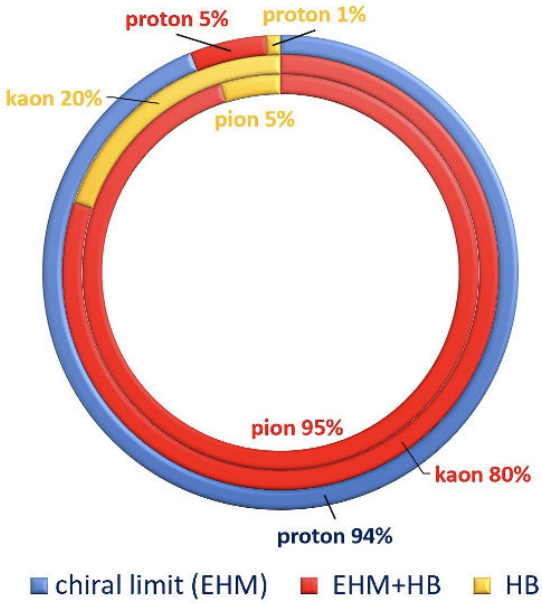

FIGURE 1. Mass budgets for the pion, kaon and proton. Figure from [1].

Based on the goal to understand more precisely these mechanisms, a broad future research program has been proposed for measurements at the CERN Super Proton Synchrotron (SPS) beamline M2, including (1) quark and gluon PDFs in the pion, kaon and proton, (2) hadron radii as a consequence of confinement, and (3) the mass spectra of excited mesons, with the Apparatus for Meson and Baryon Experimental Research (AMBER).

2. Setup and physics program

AMBER is largely based on the existing setup by the COMPASS collaboration, located in the experimental hall EHN2 in the north area of the SPS. It is planned to inherit many detector components from COMPASS, with a number of needed extensions and modernisations. The new collaboration of about 200 physicists is still in formation stage. It has a large overlap with COMPASS, but also a number of new groups

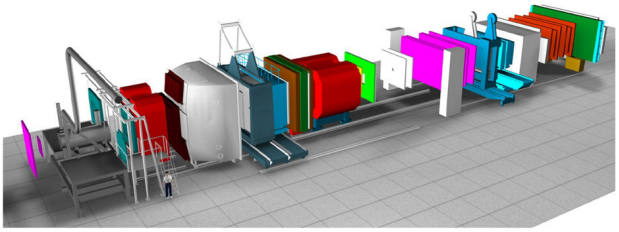

FIGURE 2. The setup of the COMPASS experiment, as planned to be largely taken over by AMBER. The beams from the SPS M2 beamline enter from the left. The target region is equipped here with the polarized target, visible as large cylindric solenoid and the L-shaped helium supply line (both in grey). It will be used, for providing a liquid-helium target, in the antiproton production measurements of AMBER.

joining the effort. The setup of AMBER is presented in Fig. 2. The core part is a two-stage magnetic spectrometer, equipped with tracking, PID and calorimetry in both stages, for measurements of reaction products in forward kinematics of collisions of the incoming beams with fixed targets. The various physics programs descibed in the following need smaller adaptions of this core setup, mostly of the target region. The large overlap of the other detector components used for all programs and the common parts for data acquisition, analysis and Monte-Carlo simulation software is the synergy driving the foundation of the collaboration. The M2 beamline currently provides the highest-energy-intensity muon beams worldwide, as well as hadron beams with energies in the range of 100 to 200 GeV.

The first Letter of Intent (LoI) [2] was worked out in the year 2017, and a proposal for the first phase of the experiment, submitted in 2018, was approved by the CERN Research Board in 2020. Longer-range plans include the idea of a major modification of the beamline, allowing for the radio-frequency separation of the different components of the hadron beam. As highlighted in the introduction, especially the kaon is of interest in that regard. Since the technological involvements for this modifications are still being worked out, measurements with the available "conventional" beams have been separated out in the Phase-1 proposal [3], allowing for an independent approval and planning procedure for measurements to take place in the years 2022 to 2028.

The program as of the LoI with muon beam included elastic muon-proton scattering at 100 GeV beam energy for a measurement of the proton form factor at low momentum transfer and the thus of the proton radius, and a continuation of the COMPASS program on Generalized Parton Distributions (GPD), with a focus on determining GPD-E in hard exclusive reactions. For the Phase-1 proposal, only the proton-radius part has been worked out. Two more measurement ideas from the LoI have been approved with the Phase-1 proposal, namely the determination of antiproton production cross-sections in proton-proton and proton-helium collisions in the energy rang 20-280 GeV, as input for dark matter search, and the determination of pion PDFs in Drell-Yan pair production employing a 190 GeV pion beam. The idea of using the comparatively high antiproton fraction of the negative hadron beam at lower beam energies of 12 to 20 GeV for heavy-quark exotics production was not followed up in the Phase-1 proposal.

The further program of the LoI intended to be worked out in a Phase-2 proposal in the near future is mainly driven by the idea to make use of a proposed future modification of the M2 beamline: By radio-frequency (rf) modulation of the beam particles, it will allow to separate the hadron beam into its species. Here, most prominently the kaon component is of interest as highlighted in the introduction. It has so far not been clarified, however, whether this technology can provide the high kaon beam intensities of up to 10^8 per second that were targeted at the time of the LoI for measurements of Drell-Yan processes providing the much desired experimental insight into the kaon PDFs. This aspect is different for the further ideas for an rf-separated kaon beam that require only smaller intensities in the range of $10^6/\mathrm{s}$. Unlike the Drell-Yan setup with a massive beam absorber between the target and the spectrometer, they are to be realized with an "open" spectrometer setting, where all interaction products and the non-deflected part of the beam enter the detector region and limit the acceptable beam rate. Intended measurements with open spectrometer are (1) kaon-induced reactions off nuclear targets at smallest momentum transfers where photon exchange dominates (Primakoff effect), for a measurement of the kaon polarisability and other low-energy constants, (2) prompt-photon production off hydrogen and nuclear targets by kaon and pion beams for constraining the gluon PDF of mesons, (3) kaon-induced spectroscopy for high-precision study of the the strange-meson spectrum, and (4) vector meson production on various nuclear targets for the determination of spin density matrix elements. All these measurements with open spectrometer are softer in terms of the beam energy requirement in the range of 50 to 100 GeV, except for the prompt-photon production which would favor a beam energy higher than 100 GeV. Recently, the idea to determine the kaon radius in kaon-electron scattering has been added to this list, with a similar kinematics as the Primakoff reactions and thus possibly combinable with this part of the program.

The key parameters of the rf-separated kaon beams, namely its energy and intensity, it currently worked out in close collaboration with with the CERN beam department. The time scale of the Phase-2 program is currently to start after the SPS Long Shutdown 4 foreseen in the year 2030.

In the following chapters, the physics topics of Phase-1 are discussed in more detail.

3. Proton radius measurement

The spatial extension of the most abundant hadron in the universe, the proton, is of key interest in many fields of science, and a benchmark parameter in the quantitative understanding of QCD when solved for the lowest-lying 3-quark bound state

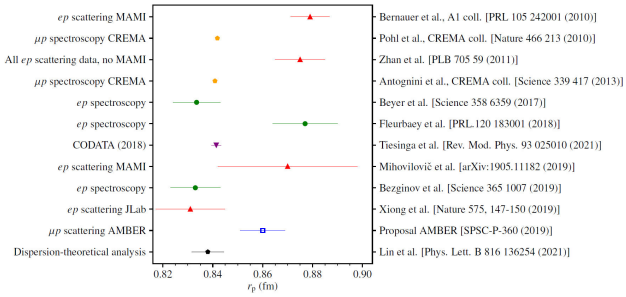

FIGURE 3. Determinations of the proton radius after 2010. The measurement with the highest experimental precision comes from transitions in muonic hydrogen atoms, as investigated by the CREMA collaboration. The most elaborate electron scattering experiment has been done by the A1 collaboration at MAMI. The upcoming AMBER measurement with high-energy muon beam aims at a similar precision as achieved in electron scattering.

by continuum or lattice methods. Since the early times of measurements of the proton radius by Hofstadter at SLAC in the late 1950ies, many measurements have been undertaken. The progress over the past 10 years is summarized in Fig. 3.

The early measurements at SLAC gave a proton radius of about 0.80 fm [4]. With the vector meson spectrum becoming known, dispersion relations could be exploited and led to the theoretically expected value for the proton radius of 0.84 fm in 1975 [5]. The precision experiment of Simon *et al.* at the Mainz accelerator [6] in 1980 resulted in 0.862 fm. The discrepancy of this experimental value with the theoretical expectation was reaffirmed in the updates of the dispersion calculations, as in Ref. [7] and recently in Ref. [8].

For clarifying this riddle from the experimental side, two main approaches were persued in the following, namely renewed electron scattering experiments on the one side, and precision experiments for atomic transitions in hydrogen and also on muonic atoms on the other side. The latter was performed by the CREMA collaboration [9] in the year 2010 and resulted in a value of 0.841 fm with extremely small experimental uncertainties, while the new experiment at MAMI by the A1 collaboration [10] gave in the same year an even larger value of 0.88 fm. The recent PRad experiment at Jefferson Lab [11] measured also the proton radius using electron scattering and determined a value of 0.83 fm, with however a noncompetitive uncertainty, such that the proton radius riddle can not be considered settled.

An experimental approach so far not realized is elastic scattering of muons at low momentum transfer. Being on theoretical description equivalent to the use of electrons, they bring the advantage of very different systematic unceratinties. Those are, *e.g.* in case of the radiative corrections, smaller and thus more favorable for the muon, and in general such a different approach is promising to point to the origin of the discrepancies discussed above. While the MUSE experiment at PSI is pursuing this idea with low-energy muon beams of up to about 200 MeV, AMBER employs the high-energy muon beam available at the M2 beamline. For exploiting the spectrometer capabilities and achieving the best resolution in

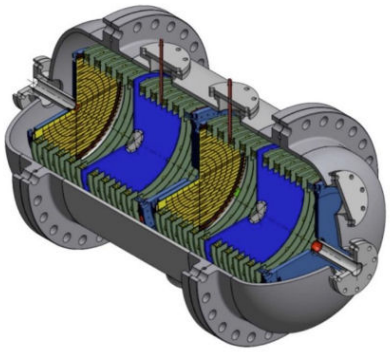

FIGURE 4. The active-target high pressure TPC for the proton radius measurement.

the target configuration discussed in the following, a beam energy of 100 GeV is chosen.

For measuring the elastic muon-proton scattering process with high purity and efficiency at such a high beam energy, is indispensable to measure in coincidence the muon scattering kinematics and the recoiling proton. At small momentum transfers, this is prohibitly difficult with a target that encloses the hydrogen even with thin walls and being separated from the detector. The technique thus employed is an active target, where the hydrogen gas is at the same time the detector volume. The ionization produced in the gas is recorded by operating the target as time-projection chamber (TPC), with appropriate high-voltage field and readout plates as depicted in Fig. 4.

This TPC will be placed in the target region of the setup, cf. Fig. 2. For the high-precision determination of the muon scattering angle, dedicated detector telescopes will be installed upstream and downstream of the TPC as sketched in Fig. 5. They will contain a combination of silicon pixel detectors (ALPIDE are foreseen) with a high spatial resolution of a few micrometers, but only a coarse timing, and fast scintillating-fiber detectors which provide time signals with a high precision better than 1 ns. The total length of the target region is about 9 meters, and the space between the tracking stations is equipped with helium lines in order to minimize the effect of multiple scattering.

With this setup, the goal is to collect a sample of 70 million elastic muon-proton scattering events in the momentum transfer Q^2 range from 0.001 to 0.04 GeV^2. This will take about one beamtime of 140 days, currently foreseen for the

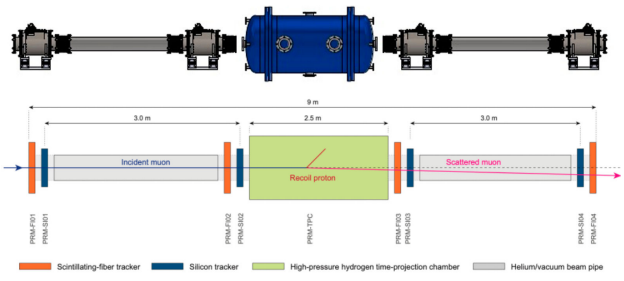

FIGURE 5. The active-target high pressure TPC for the proton radius measurement.

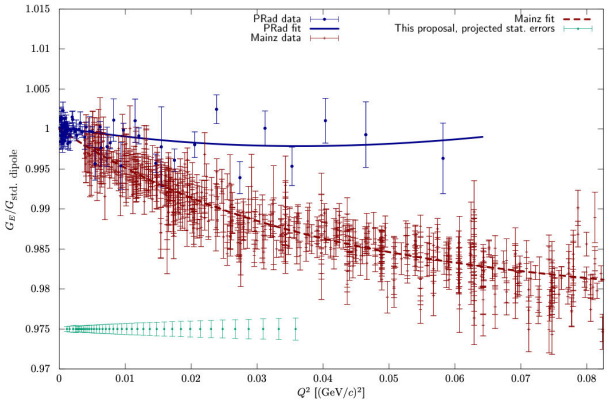

FIGURE 6. The uncertainty projections of the AMBER experiment, indicated by the green data points arbitrarily placed at a fixed value 0.975 of the proton form factor ratio $G_E/G_{std.dip}$. It has competitive precision as compared to the data points available for the Mainz [10] and PRad data [11].

year 2023. From these data, we aim at determining the Q^2 dependence of the proton form factor as indicated in Fig. 6.

From such data, it will be possible to determine the proton radius with a precision of about 0.01 fm. The TPC technique in the high-energy beam environment of the M2 beamline has been first explored in a parasitic measurement in the muon halo downstream of COMPASS in autumn of 2018. In the mean time, a dedicated test beam time in October 2021 has further proven the principle of the measurement. The detector components, including the large TPC shown in Fig. 4, are still in the development phase.

4. Antiproton production cross sections

Including the AMS-02 data [12, 13], the antiparticle flux in the cosmic rays is now known with a few-percent precision. Two processes are thought of being their origin: The standard-model interactions of protons on the interstellar matter, and dark matter interactions. For concluding on a possible dark-matter contribution, the standard-model part must be estimated as precise as possible. As it is indicated in Fig. 7, the antiproton spectra are known with a much higher experimental precision than the uncertainties steming from the astrophysical model and, for part of the spectrum being largest, the uncertainty from the particle cross sections.

Thus providing the needed cross sections with higher precision will allow to further interpret the astrophysical data. For covering the respective kinematics, AMBER foresees measurements with proton beams from a few ten GeV up to 250 GeV, and in the pseudo-rapidity range of produced particles from 2.4 to 5.6. The cross section of antiproton production will be determined differential in momentum and pseudo-rapitidy in proton-hydrogen and proton-helium collisions.

The impact on constraining the production mechanisms of cosmic antiprotons is indicated in Fig. 8 for collisions with protons, and in Fig. 9.

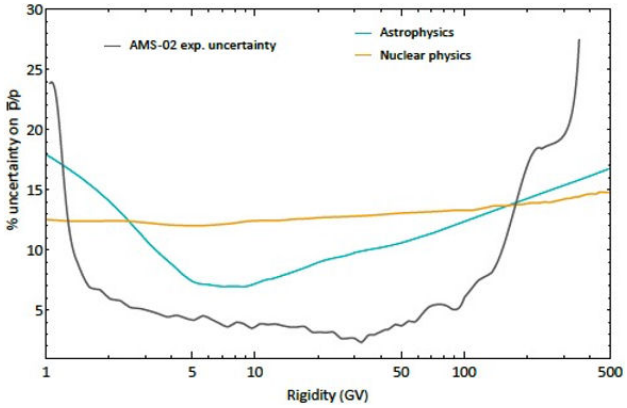

FIGURE 7. Comparison of the precision by which the antiproton flux is known to astrophysical and nuclear physics uncertainties.

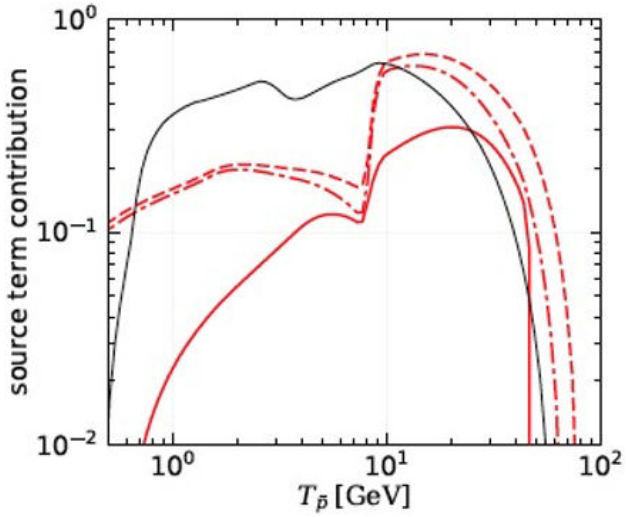

FIGURE 8. Impact of the planned AMBER data on constraining possible sources of cosmic antiproton production in $p-p$-collisions. Further explanations in the text.

In Fig. 8, the red curves are for the planned AMBER data for different covered energy ranges, compared to NA61 with beam energies in the range 20 to 158 GeV. The continuous red line is for measurements with beam energies 100 to 190 GeV, the dash-dotted line for 50 to 190 GeV, and the dashed curve for 50 to 250 GeV. For $p-p$ collisions, only for the highest energies an additional kinematic coverage ca be achieved.

For collisions with helium, as presented in a similar way in Fig. 9, the competing experiement is LHCb. Here, AMBER can deliver new and exclusive information over a much broader range.

A first test run for the antiproton production measurements with AMBER are foreseen in 2022, linked to the COMPASS beam time.

5. Pion-induced Drell-Yan processes

As indicated in the introduction, the inner quark-gluon structure of pions and kaons is of high interest in QCD. As investigated *e.g.* in Ref. [14], the respective distribution functions

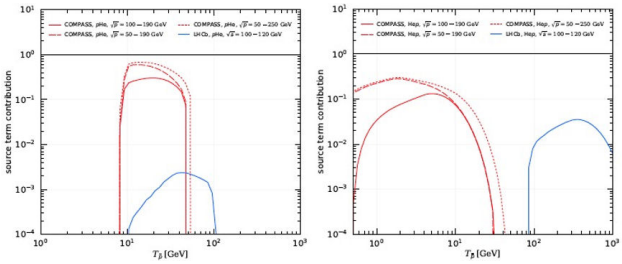

FIGURE 9. Same as Fig. 8, here for $p-$He (left) and He $-p$ (right) collisions.

Experiment	Target type	Beam energy (GeV)	Beam type	Beam intensity (part/sec)	DY mass (GeV/c^2)	DY events
E615	20 cm W	252	π^+ π^-	17.6×10^7 18.6×10^7	4.05 – 8.55	5000 30000
NA3	30 cm H_2	200	π^+ π^-	2.0×10^7 3.0×10^7	4.1 – 8.5	40 121
	6 cm Pt	200	π^+ π^-	2.0×10^7 3.0×10^7	4.2 – 8.5	1767 4961
NA10	120 cm D_2	286 140	π^-	65×10^7	4.2 – 8.5 4.35 – 8.5	7800 3200
	12 cm W	286 194 140	π^-	65×10^7	4.2 – 8.5 4.07 – 8.5 4.35 – 8.5	49600 155000 29300
COMPASS 2015 COMPASS 2018	110 cm NH_3	190	π^-	7.0×10^7	4.3 – 8.5	35000 52000
This exp	75 cm C	190	π^+	1.7×10^7	4.3 – 8.5 4.0 – 8.5	21700 31000
		190	π^-	6.8×10^7	4.3 – 8.5 4.0 – 8.5	67000 91100
	12 cm W	190	π^+	0.4×10^7	4.3 – 8.5 4.0 – 8.5	8300 11700
		190	π^-	1.6×10^7	4.3 – 8.5 4.0 – 8.5	24100 32100

Isoscalar target + *Both positive and negative beams* + *High statistics*

FIGURE 10. The proposed measurements of Drell-Yan processes at AMBER, compared to previous measurements.

are heavily dependent on the model approach and need experimental inputs as constraints. For the pion structure, experimental data are scarce, with only a poor knowledge of the valence quark distributions, and the sea and gluon distributions are basically unknown. It is experimentally much more difficult to investigate hard lepton-quark or quark-quark collisions for the pion, which can not be provided as a fixed target as it is possible for the nucleon. The previous experiments NA3 [15], NA10 [16] and E615 [17] have mostly taken data with heavy nuclear targets and thus are affected by large nuclear effects, and partly there is no information about the absolute cross sections available. E615 and NA3 have measured with both π^- and π^+ beams, but only NA3 used the data to separate sea and valence quark contributions. There are unexplained discrepancies between the NA10 and E615 data, which are old and there is no way to reanalyse them with modern approaches.

The projected measurements of AMBER with onventional beams are summarized as presented in Fig. 10.

With employing C targets being isoscalar, systematic uncertainties are minimized as compared to the previously used heavy targets. The new measurement shall measure both signs of the pion charge, and collect also high statistics for π^+. The expected accuracy as compared to the available NA3 data is shown in Fig. 11.

From these data, together with those for negative beam charge, the sea-over-valence quark distribution can be determined. In Fig. 12, the projected uncertainties are compared

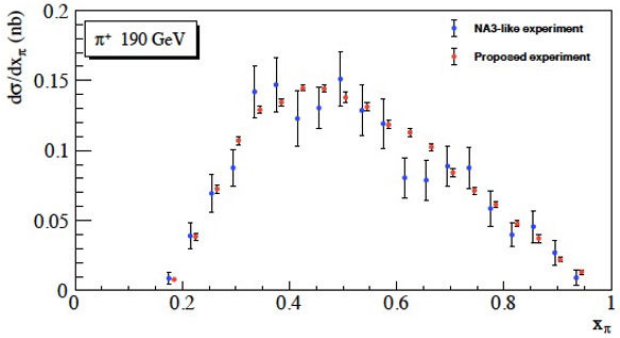

FIGURE 11. The Drell-Yan cross section for 190 GeV positive pions depending on x_π.

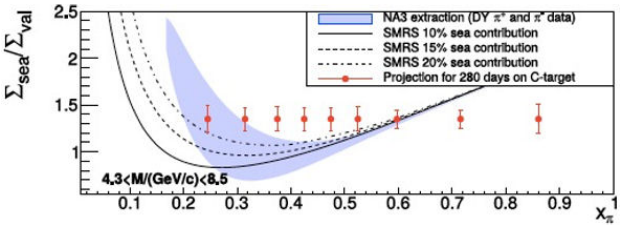

FIGURE 12. The Drell-Yan cross section for 190 GeV positive pions depending on x_π.

Experiment	Target type	Beam energy (GeV)	Beam type	J/ψ events
NA3 [76]	Pt	150	π^-	601000
		280	π^-	511000
		200	π^+	131000
			π^-	105000
E789 [129, 130]	Cu	800	p	200000
	Au			110000
	Be			45000
E866 [131]	Be Fe Cu	800	p	3000000
NA50 [132]	Be	450	p	124700
	Al			100700
	Cu			130600
	Ag			132100
	W			78100
NA51 [133]	p	450	p	301000
	d			312000
HERA-B [134]	C	920	p	152000
COMPASS 2015 COMPASS 2018	110 cm NH_3	190	π^-	1000000 1500000
This exp	75 cm C	190	π^+	1200000
			π^-	1800000
			p	1500000
	12 cm W	190	π^+	500000
			π^-	700000
			p	700000

FIGURE 13. The achievable number of J/ψ events, n for 190 GeV positive pions depending on x_π.

to the constaint from the NA3 analysis and different phenomenological sea contributions.

Along with pure Drell-Yan muon pairs above 4.3 GeV invariant mass, a high statistics of J/ψ production will be recorded in the same data set, as compared to the available statistics from other experiments in Fig. 13. Studying the x_F

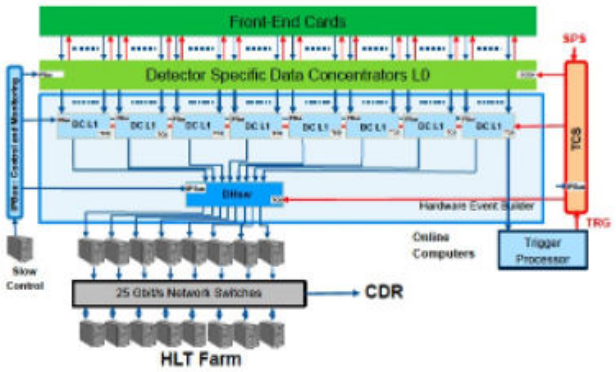

FIGURE 14. The free-running data acquisition scheme. The detector frontends do not receive a trigger signal, as in the currently existing DAQ system.

of the J/ψ production cross section allows to conclude on the production mechanisms, gg fusion versus $q\bar{q}$ annihilation. This allows to probe the gluon and quark PDFs of the pion. A respective study is published in Ref. [18].

In addition the signal of the $\Psi(2S)$ resonance is contained in the data, with the advantage of being free of the feed-down from the production of χ_{c1} and χ_{c2}.

6. Hardware developments

Various upgrades are planned and are partly already started, in order to cope with the challenges of the future measurements.

Most prominently, the data acquisition is foreseen to be transformed into a free-running mode, where no low-level trigger signal is needed anymore. Evidently, all detector frontend systems have to be capable of delivering their information in such a triggerless mode, which requires modifications for most detector readout systems. This kind of readout scheme, as sketched in Fig. 14, is needed first for the proton radius measurement, where the generation of an efficient trigger signal turned out to be difficult and the existing DAQ system from COMPASS is limited at a rate of 50 kHz. The free-running DAQ, in turn, will allow to buffer all data induced by the 2 MHz beam and thus to apply sophisticated data selection criteria with large latency, even in the order of hours. The key idea is to slice the detector information in time segments that will allow later to find signals belonging to equal time. Clearly, for detectors not having an own intrinsic time resolution, these time slices have to be larger than for detectors with a precise time resolution. The TPC is such a slow detector, whose signals can only be correctly interpreted when combined at a later stage with the time information of fast detectors.

For the tracking detectors, new developments are large-size pixelGEM and large-area micro-pattern gaseous detectors (MPGD). The future Drell-Yan program requires high-rate capable CEDAR detectors for beam particle identification. For the longer-range strange-meson spectroscopy program, a new RICH detector for lowest particle momenta would be needed to extend the accessible phase space with particle identification. Such a RICH-0 has to be installed upstream of the first spectrometer magnet.

1. C. Roberts, *Emergent hadron mass*, STRONG2020 Newsletter 3, April 2021, `http://www.strong-2020.eu/news-documents/newsletter.html?download=4:newsletter-march-2021`.
2. Letter of Intent: A New QCD facility at the M2 beam line of the CERN SPS (COMPASS++/AMBER), submitted August 2018, arXiv:1808.00848.
3. COMPASS++/AMBER: Proposal for Measurements at the M2 beam line of the CERN SPS Phase-1: 2022-2024, CERN-SPSC-2019-022; SPSC-P-360, submitted May 2019. `http://cds.cern.ch/record/2676885`.
4. E. E. Chambers and R. Hofstadter, Structure of the Proton, *Phys. Rev.* **103** (1956) 1454-1463.
5. G. Höhler *et al.*, Analysis of electromagnetic nucleon form factors, *Nuclear Physics B* **114** (1976) 505-534.
6. G. G. Simon *et al.*, Absolute electron-proton cross sections at low momentum transfer measured with a high pressure gas target system, *Nuclear Physics A* **333** (1980) 381-391.
7. P. Mergell, U. G. Meissner, D. Drechsel, Dispersion theoretical analysis of the nucleon electromagnetic form-factors, *Nucl. Phys. A* **596** (1996) 367-396.
8. Y. Lin *et al.*, High-precision determination of the electric and magnetic radius of the proton, *Phys. Lett. B* **816** (2021) 136254.
9. R. Pohl *et al.*, The size of the proton, *Nature* **466** (2010) 213.
10. J. C. Bernauer *et al.*, High-Precision Determination of the Electric and Magnetic Form Factors of the Proton, *Phys. Rev. Lett.* **105** (2010) 242001.
11. W. Xiong *et al.*, A small proton charge radius from an electron-proton scattering experiment, *Nature* **575** (2019) 147-150.
12. M. Aguilar *et al.*, First Result from the Alpha Magnetic Spectrometer on the International Space Station: Precision Measurement of the Positron Fraction in Primary Cosmic Rays of 0.5-350 GeV, *Phys. Rev. Lett.* **110** (2013) 141102.
13. M. Aguilar *et al.*, Antiproton Flux, Antiproton-to-Proton Flux Ratio, and Properties of Elementary Particle Fluxes in Primary Cosmic Rays Measured with the Alpha Magnetic Spectrometer on the International Space Station, *Phys. Rev. Lett.* **117** (2016) 091103.
14. L. Chang and C. D. Roberts, Regarding the distribution of glue in the pion, `https://arxiv.org/abs/2106.08451`.
15. J. Badier *et al.*, Experimental Determination of the pi Meson Structure Functions by the Drell-Yan Mechanism, *Z. Phys. C* **18** (1983) 281.

16. B. Betev *et al.*, Observation of Anomalous Scaling Violation in Muon Pair Production by 194 GeV/c π^- Tungsten Interactions, *Z. Phys. C* **28** (1985) 15.

17. J. S. Conway *et al.*, Experimental Study of Muon Pairs Produced by 252-GeV Pions on Tungsten, *Phys. Rev. D* **39** (1989) 92-122.

18. C. Hsieh, Y. Lian *et al.*, NRQCD analysis of charmonium production with pion and proton beams at fixed-target energies, *Chinese Journal of Physics*, **73** (2021) 13-23.